

U–Pb LA-ICP-MS geochronology of polygenetic zircons from Beshta and Kamenistaya intrusions (the Greater Caucasus)

David Shengelia¹  · Leonid Shumlyanskyy^{2,3}  · Giorgi Chichinadze¹ 
Tamara Tsutsunava¹  · Giorgi Beridze¹  · Irakli Javakhishvili¹ 

Received: 25 May 2022 / Revised: 5 July 2022 / Accepted: 14 July 2022 / Published online: 20 August 2022
© The Author(s), under exclusive licence to Science Press and Institute of Geochemistry, CAS and Springer-Verlag GmbH Germany, part of Springer Nature 2022

Abstract The Beshta–Kamenistaya intrusions are located in the Main Range structural zone of the Greater Caucasus. They are composed of tonalitic gneisses that genetically resemble granites of the tholeiitic series of the ophiolitic complexes. The Beshta–Kamenistaya orthogneisses and associated rocks of the nappes differ markedly from those of the Main Range zone. All of them were overthrust to the Main Range zone during the Bretonian orogeny. The age of their protolith and the metamorphism are still not defined. Using the zircon U–Pb LA-ICP-MS dating two age populations of zircons have been distinguished in the rocks of the Beshta–Kamenistaya intrusions. The age of the main population of zircons from orthogneisses is 426–300 Ma. Several age groups can be distinguished in this population. The main group yielded a Concordia age of 386.9 ± 1.4 Ma. There are also smaller peaks at 409–405, 375–373, and 351 Ma. The oldest ages (426–395 Ma) were detected in the core parts of the complex crystals. We assume that the crystallization of the parental for orthogneisses rocks (tonalities) took place at 410–395 Ma, whereas the Concordia age of 386.9 ± 1.4 Ma and a peak at 375–373 Ma correspond to the metamorphic event. The whole metamorphic cycle, including progressive and regressive stages, occurred between 395 and 370 Ma.

Zircons, dated in the Beshta–Kamenistaya intrusion at 350 Ma and younger, correspond to the Late Variscan orogeny. Zircons dated 3102–2769 Ma represent xenocrysts captured by the melts during their formation from the ancient rocks in the crystalline basement.

Keywords The Greater Caucasus · Magmatism · Metamorphism · Orthogneisses · U–Pb zircon dating

1 Introduction

The Beshta and Kamenistaya massifs are exposed in the Pass subzone of the Main Range structural zone of the Greater Caucasus (Fig. 1) and represent a component of the Laba metamorphic complex. This area is characterized by a complex geological structure.

It should be noted that the crust in the Greater Caucasus is tectonically layered. Since the early 1970s, the identification of the nappe structure of both the Alpine cover and pre-Alpine basement in many of its zones, including the Greater Caucasus Main Range zone, has been of great importance (e.g., Gamkrelidze 1980; Baranov and Grekov 1982; Adamia 1984; Gamkrelidze et al. 1996, 2020). It has been found that tectonic layering occurs in the crust of the entire central segment of the Mediterranean belt. As a result of studies in the Greater Caucasus, the presence of both large and small allochthonous structures has been established. The above-mentioned Laba complex of the Pass structural subzone of the Greater Caucasus is also characterized by the nappe structure.

The allochthonous nature of the Lashtrak and Adjarka “suites” (e.g., Baranov and Kropachev 1976; Adamia 1984; Shengelia et al. 1989), as well as of the associated

✉ Tamara Tsutsunava
tamara.tsutsunava@tsu.ge

¹ Al. Janelidze Institute of Geology of Iv. Javakhishvili Tbilisi State University, Tbilisi, Georgia

² School of Earth and Planetary Sciences, Curtin University, Perth, Australia

³ M.P. Semenenko Institute of Geochemistry, Mineralogy and Ore Formation, Kyiv, Ukraine

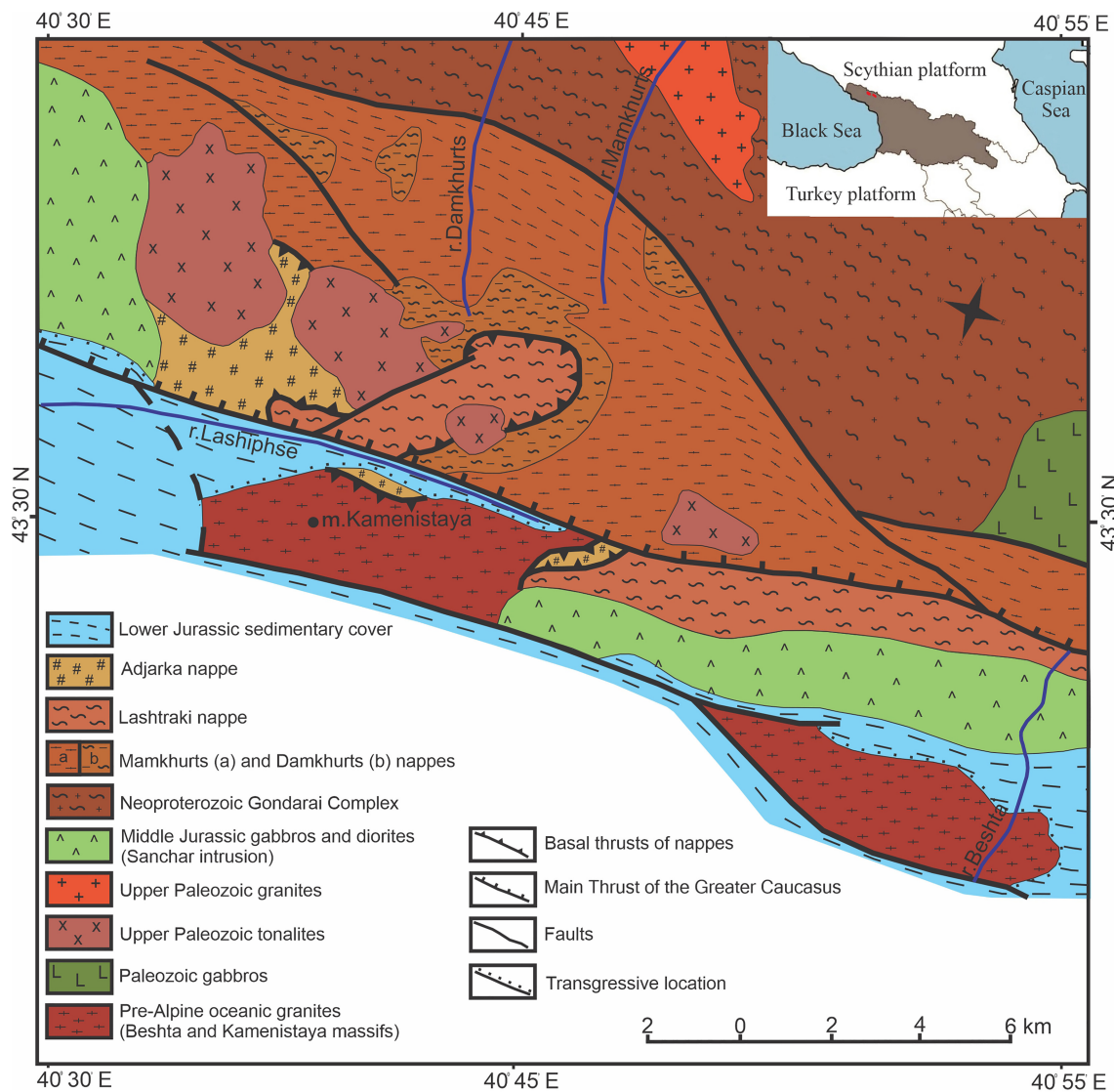


Fig. 1 A schematic geological map of the Laba metamorphic complex (Somin 1971, with additions by the authors)

orthogneisses of the Beshta and Kamenistaya massifs, has been defined (Shengelia et al. 1989). All these differ sharply from other metamorphic rocks in the Main Range structural zone in terms of the geological position, petrographical, mineralogical, and geochemical features of the rocks, as well as the nature of metamorphism. Even though the petrology and geochemistry of the Beshta and Kamenistaya rocks are reasonably well studied, the age of their protolith and the timing of metamorphic events have not yet been defined. In contrast, the age of granitoids in the Main Range zone has been determined quite accurately (Gamkrelidze et al. 2020).

The article aims to define the U–Pb LA-ICP-MS zircon age of the Beshta and Kamenistaya intrusions. The obtained results allow us to better define the connection

between the studied granitoids and pre-Alpine igneous rocks of the Main Range structural zone.

1.1 Geological setting

Orthogneisses of the Beshta and Kamenistaya intrusions are exposed at the southern slope of the Greater Caucasus in the Beshta and Lashipse river gorges (Fig. 1). They are mostly in transgressive contact with the early Jurassic sediments, although in places the contact is tectonic. The Kamenistaya intrusion in its northern and eastern parts contacts the Adjarka and Lashtrak nappes. This massif is cut by the Middle Jurassic Sanchar intrusion. The Beshta and Kamenistaya orthogneisses spatially associate with the Adjarka and Lashtrak nappes, hornblende-bearing gneisses, amphibolites, and serpentinized ultrabasic rocks. The latter

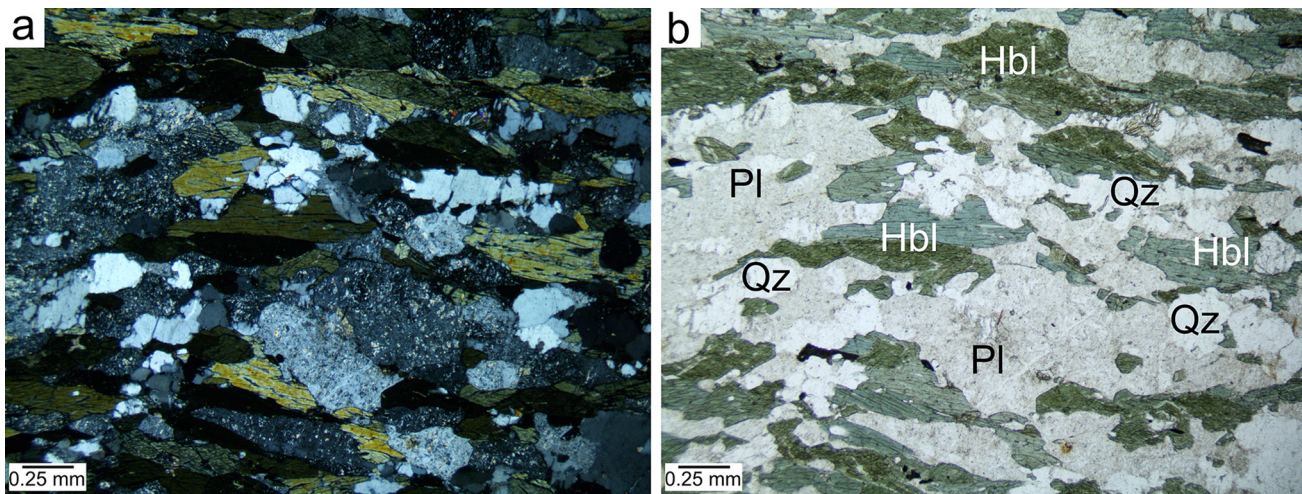


Fig. 2 Hornblende-bearing tonalitic gneiss. **a** PPL and **b** XPL (PPL plane polarized light and XPL crossed polarized light)

shares a similar history of geological development with the orthogneisses (Shengelia et al. 1989). The Laba (Dankhurts and Mamkhurts nappes) and the Gondarai metamorphic complexes are located to the north of the Beshta and Kamenistaya intrusions.

Orthogneisses of the Beshta and Kamenistaya massifs share similar composition and comprise tonalite gneisses. Diorite-gneisses and gabbro-diorite-gneisses are rare rock types and have gradual contact with tonalites. These rocks are intensely chloritized, epidotized, and granulated. Orthogneisses have the following mineral composition: plagioclase, chlorite, epidote group minerals, quartz, green hornblende, actinolite, and garnet. Accessory minerals are zircon, apatite, titanite, and opaque. Rarely, fresh green hornblende is observed, it is often replaced by light blue hornblende, epidote, and chlorite (Fig. 2). Plagioclase is saussuritized and prehnitized. Garnet occurs as intact porphyroblasts (Fig. 3) and disintegrated grains, where chlorite fills in the space between the fragments (Fig. 4). The electron microprobe analysis has revealed the following mineral parageneses in orthogneisses (Shengelia 1987):

$$\text{Hbl}_{43} + \text{Pl} + \text{Grt}_{77-69} \pm \text{Qz},^1 \quad \text{Grt}_{69-77} + \text{Chl}_{36-49} + \text{Act}_{43} + \text{Pl}^{19} \pm \text{Ep} \pm \text{Hbl}_{53} + \text{Qz},$$

$$\text{Grt}_{68-78} + \text{Chl}_{30-33} + \text{Pl}^{37} + \text{Ep} + \text{Ca} + \text{Qz}.$$

The mineral parageneses of the Beshta and Kamenistaya orthogneisses are similar to those found in metamorphosed basic rocks of the Lashtrak nappes. Concerning the chemical composition, orthogneisses of the Beshta-Kamenistaya massifs are genetically close to granites of the tholeiitic series that occur in the upper part of the ophiolitic complexes. The latter is formed as a result of the partial

melting of the oceanic crust and represents the final product of the differentiation of the basaltic magma (Coleman 1977; Shengelia et al. 1989).

The Lashtrak and Adjarka nappes are composed of micaceous and amphibole schists of various compositions, albite-quartz porphyroids, and quartzites. Marbles having a thickness of up to several tens of meters are observed at the marginal parts of the plates. They host post-Early-Ordovician crinoids (Potapenko and Stukalina 1971). Rocks of the Lashtrak and Adjarka nappes underwent regional metamorphism of the epidote–amphibolite facies and kyanite–sillimanite baric type.

The Beshta–Kamenistaya orthogneisses, as well as rocks of the Lashtrak and Adjarka nappes, differ sharply in their origin, composition, and metamorphic nature from the magmatic and metamorphic formations of the Main Range structural zone of the Greater Caucasus. In our opinion, some of them represent fragments of the ophiolitic complex. The allochthonous nature of the Lashtrak and Adjarka “suites” has been established by Baranov and Kropachov (1976) and Adamia (1984). The authors of this article, based on a number of lines of evidence, also accept the allochthonous nature of the Beshta and Kamenistaya massifs. It has been suggested that the Beshta and Kamenistaya orthogneisses and rocks of the Lashtrak and Adjarka nappes have simultaneously undergone moderate and presumably higher-pressure regional metamorphism ($T = 420\text{--}465^\circ\text{C}$, $P=5.2\text{ kbar}$) before the overthrusting (Shengelia et al. 1989). Supposedly, during the Bretonian orogeny, they were thrust over the Pass subzone of the Main Range zone of the Greater Caucasus, to the area of low pressure ($P \approx 1.5\text{--}3.3\text{ kbar}$; Shengelia 1987; Shengelia and Hatar 1989; Korikovsky et al. 1991) metamorphism (Shengelia et al. 1989). Some researchers (Zaridze and Shengelia 1977, 1978a, b) assumed the higher-pressure

¹ Mineral symbols are given as per Whitney and Evans (2010). Index numbers of dark-colored minerals indicate their magnesium numbers [$\text{Mg}/(\text{Mg} + \text{Fe}^{2+})$]; Index numbers of Pl are the content of the anorthite molecule (mass%).

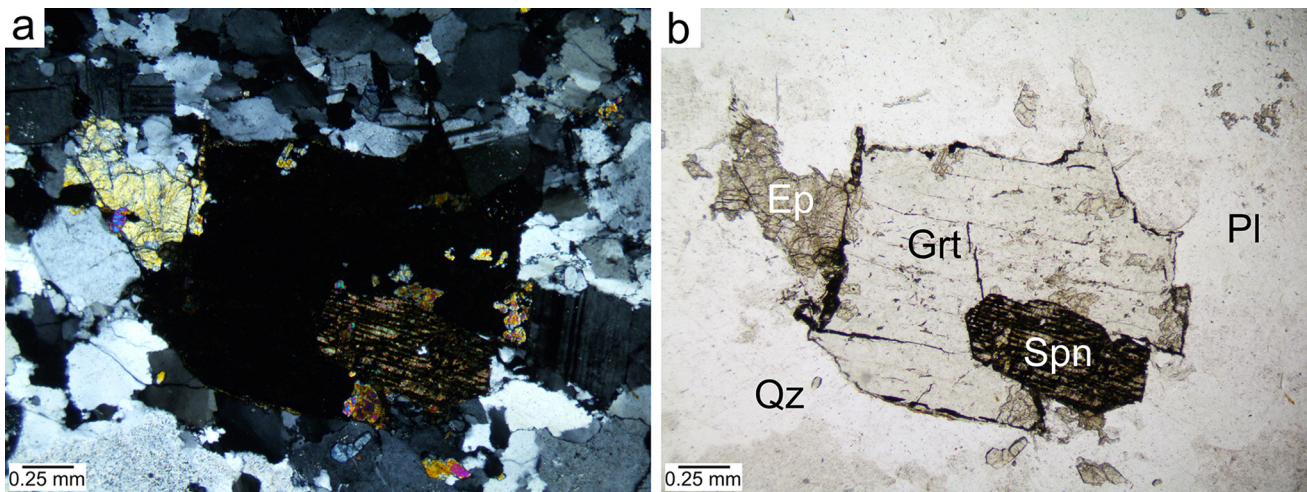


Fig. 3 Fresh garnet in tonalitic gneiss. **a** PPL and **b** XPL

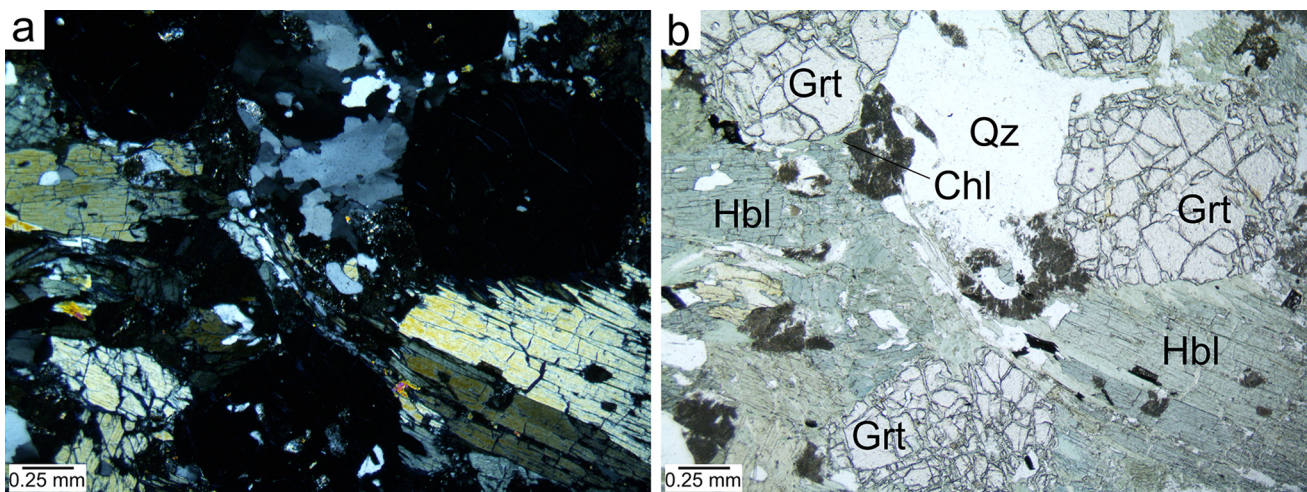


Fig. 4 Disintegrated and chloritized garnet in the hornblende gneiss. **a** PPL and **b** XPL

conditions of metamorphism of the rocks composing the Lashtrak and Adjarka nappes, where kyanite and staurolite-bearing associations occur. The incipient rocks were represented by primary miopelagic and chemogenic sediments, apparently formed in deep water oceanic conditions. It should be noted that metamorphic rocks of the Kiafara nappe thrust over the Greater Caucasus Fore-range structural zone (Baranov and Grekov 1982; Shengelia and Ketskhoveli 1982; Shengelia et al. 1984; 1986; Somin 2011) is similar to the Lashtrak nappe.

1.2 Analytical methods

Zircon crystals were extracted from the crushed samples using standard separation techniques (shaking table, magnetic separation, and heavy liquids) at the M.P. Semenenko Institute of Geochemistry, Mineralogy and Ore Formation, Kyiv, Ukraine. Hand-picked under optical microscope

crystals were mounted in epoxy resin and polished to expose the internal parts of the crystals. U–Pb isotopic data were collected using laser ablation inductively coupled plasma mass spectrometry (LA-ICP-MS). Zircon was ablated using a COMPex 102–193 nm excimer UV laser coupled to an Agilent 8900 QQQ mass spectrometer. Following 30 s of background analysis, samples were spot ablated for 30 s at 5 Hz using a 38 μm beam and laser energy at the sample surface of 2 J cm^{-2} . The sample cell was flushed with ultrahigh purity He and N₂ and high purity Ar was employed as the plasma carrier gas. Zircon standard GJ1 (601.2 ± 0.4 Ma; Jackson et al. 2004) was utilized as the primary reference material and analyzed in blocks with secondary standards Plešovice (337.13 ± 0.37 Ma; Sláma et al. 2008) and OGC (3465 ± 0.6 Ma; Stern et al. 2009). Standard blocks were inserted between every 20 unknowns. The secondary standards yielded weighted mean $^{207}\text{Pb}/^{206}\text{Pb}$ ages

and $^{238}\text{U}/^{206}\text{Pb}$ ages within an uncertainty of the recommended values.

Trace element and Hf isotope data were acquired at the John de Laeter Centre, Curtin University, using a LASS NPII + 7700 + SE Resolution excimer laser operating at the following conditions: spot size 38 micron, laser frequency 10 Hz, and energy 3 j/cm². The Hf isotope composition was measured on a Nu Plasma II mass-spectrometer. All isotopes (^{180}Hf , ^{179}Hf , ^{178}Hf , ^{177}Hf , ^{176}Hf , ^{175}Lu , ^{174}Hf , ^{173}Yb , ^{172}Yb , and ^{171}Yb) were counted on the Faraday collector array. The ^{176}Yb and ^{176}Lu values were removed from the 176-mass signal using $^{176}\text{Yb}^{173}\text{Yb} = 0.7962$ and $^{176}\text{Lu}^{175}\text{Lu} = 0.02655$ with an exponential law mass bias correction assuming $^{172}\text{Yb}^{173}\text{Yb} = 1.35274$. The interference-corrected $^{176}\text{Hf}^{177}\text{Hf}$ was normalized to $^{179}\text{Hf}^{177}\text{Hf} = 0.7325$ (Patchett and Tatsumoto 1980) for mass bias correction. Zircon crystals from the Mud Tank carbonatite were analyzed together with the samples in each session to monitor the accuracy of the results. Zircons 91500, Plešovice, GJ-1, and R33 were also run as secondary reference standards. All reference material yielded $^{176}\text{Hf}^{177}\text{Hf}$ ratios within an uncertainty of their respective reported values. Calculation of initial $^{176}\text{Hf}^{177}\text{Hf}$ and ϵHf values for unknown zircons employed the accepted ages of their zircon crystallization, a $\lambda^{176}\text{Lu}$ decay constant of 1.867×10^{-11} (Söderlund et al. 2004), and a present-day Chondritic Uniform Reservoir (CHUR) $^{176}\text{Hf}^{177}\text{Hf} = 0.282785$ and $^{176}\text{Lu}^{177}\text{Hf} = 0.0336$ (Bouvier et al. 2008).

Trace element data were collected simultaneously with Hf isotope data. Zircon standard GJ-1 was utilized as the primary reference material for concentration determination and to correct for instrument drift, using ^{91}Zr as the internal reference isotope and assuming 43.14% Zr in the unknowns. NIST SRM 612 was run as a secondary standard and yielded recommended values within 3% for all elements.

2 Results

Zircons from two orthogneiss samples representing the Kamenistaya (sample 426-3) and Beshta (sample 9-3) massifs have been analyzed for U–Pb ages (Supplement 1), Hf isotopes (Supplement 2), and trace element abundances (Supplement 3). Both samples contain two zircon populations that drastically differ in terms of their appearance and U–Pb age. The main population (85%) includes long-prismatic to short-prismatic, euhedral to subhedral colorless crystals (Fig. 5). These zircons have bright colours in CL images and reveal well-defined oscillatory zoning. The indistinct cores were noticed in several grains. Many of the grains are rimmed by bright thin mantles. The second

population is less abundant (15%) and represented by prismatic grains with rounded crystal tips. These crystals have a pronounced brown color and look very dark on CL images.

Two zircon populations have revealed very distinct U–Pb isotope ages. Zircons belonging to the smaller population yielded Archean ages varying between ca. 3100 and 2650 Ma (Fig. 6). In contrast, zircons representing the main population range in age from ca. 420 to 300 Ma. Both samples have a prominent spike at 394–386 Ma (Fig. 6). The concordant results (44 analyses) belonging to this spike yielded a Concordia age of 386.9 ± 1.4 Ma (MSWD = 6.6). There is also a series of smaller peaks at 409–405, 375–373, and 351 Ma. The youngest age obtained for the sample 426-3 is 326 ± 7 Ma (Supplement 1). Differently from this result, a group of young ages ranging from 314 to 303 Ma were obtained for the sample 9-3. It must be noted, that when several analyses were performed within a single zircon crystal, the results obtained for the marginal parts were generally younger than the ages in the central parts.

The Archean zircon population demonstrates large variability of ϵHf values calculated at the age of zircon crystallization (Fig. 7, Supplement 2). Two oldest (> 3000 Ma) zircons have negative (down to –4) ϵHf values, whereas zircons dated between 2800 and 3000 Ma have predominantly positive ϵHf values. All, except one, zircons of the young population have strongly depleted ϵHf values (> +12), reaching depleted mantle values of +16. These zircons do not reveal any systematic variations of the Hf isotope composition with age. Single zircon grain belonging to the young population has less radiogenic Hf isotope composition ($\epsilon\text{Hf} = 4.3$).

The Archean population of zircons has high concentrations of U (average 940 ppm) and Th (average 360 ppm, Supplement 3). The average Th/U ratio is 0.49. These zircons also have relatively high concentrations of LREE (average concentration of La = 24 ppm), and low concentrations of HREE (average concentration of Yb = 370 ppm). As a result, the fractionation of REE is relatively low ($\text{Yb/La}_N = 188$). Positive Ce and negative Eu anomalies are very low (Fig. 8).

In contrast, zircons belonging to the younger populations in both studied samples have much lower concentrations of U (average 330 ppm in sample 426-3 and 575 in sample 9-3) and Th (average 140 ppm in sample 426-3 and 125 in sample 9-3). The average Th/U ratio equals 0.49 in zircons from sample 426-3, and 0.32 in zircons from sample 9-3. However, the value of this ratio depends on the age of the zircon, the youngest spots (sample 9-3) yielded a Th/U ratio below 0.1. Zircon from the studied two samples differs sharply in terms of REE pattern. Zircons from sample 426-3 have a flat pattern of light and middle REE,

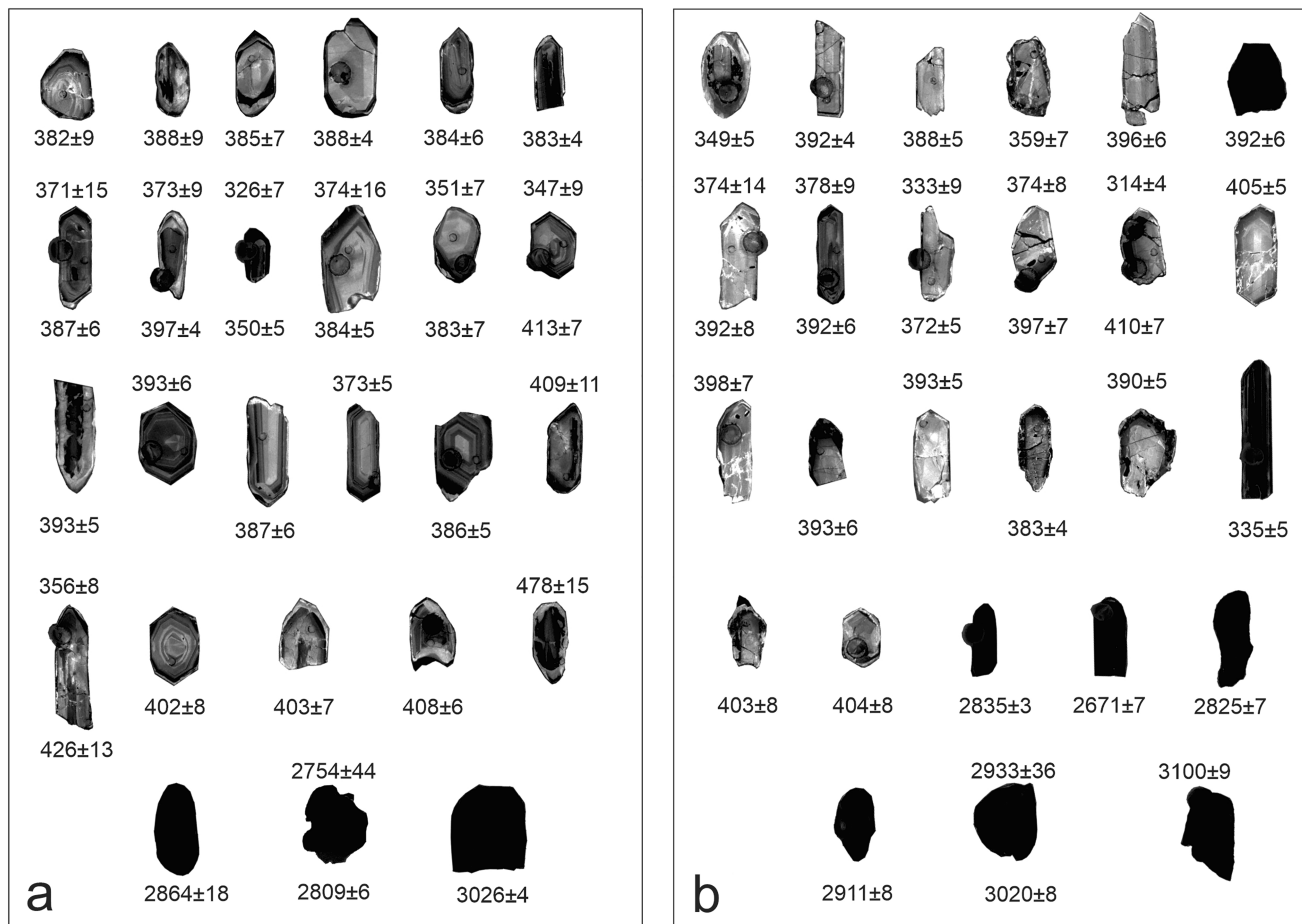


Fig. 5 CL images of analyzed zircons from samples 426-3 (a) and 9-3 (b)

with very weak positive Ce and negative Eu anomaly, whereas HREE reveals strong differentiation. The average $(\text{Yb/La})_N$ in zircon from this sample equals 82,250. In contrast, REE pattern in zircon from sample 9-3 is much more differentiated, with the average $(\text{Yb/La})_N = 195,500$. Moreover, zircon from this sample has pronounced positive Ce anomaly and moderate negative Eu anomaly.

3 Discussion

Two zircon populations have been distinguished in orthogneisses of the Beshta-Kamenistaya massif. The main population embraces zircon crystals that yielded U-Pb ages in the range of ca. 426–300 Ma, and reveal close links with igneous and metamorphic processes. Several age groups can be distinguished in this population. The main group yielded a Concordia age of 386.9 ± 1.4 Ma. There are also smaller peaks at 409–405, 375–373, and 351 Ma. The oldest ages (426–395 Ma) were detected in the core parts of the complex crystals. We assume that the crystallization of the parental for orthogneisses rocks (tonalities) took

place at 410–395 Ma, whereas the Concordia age of 386.9 ± 1.4 Ma and a peak at 375–373 Ma correspond to the metamorphic event. The whole metamorphic cycle, including progressive and regressive stages, occurred between 395 and 370 Ma.

The overthrusting of the Beshta-Kamenistaya orthogneisses and associated rocks took place during the Bretonian orogeny, at 360–350 Ma. Potapenko and Stukalina (1971) defined the age of the rocks composing the Lastrak and Adjarka nappes as post-Early Ordovician. We assume, that Beshta-Kamenistaya orthogneisses and rocks composing the Lastrak and Adjarka tectonic plates experienced metamorphism together before overthrusting to the area of the Main Range zone of the Greater Caucasus, i.e., before 350 Ma. Later they are intruded by Sudetic granites. It should be noted that by the K-Ar method for rocks of the Kiafara nappe, which is analogous to the Lashtrak nappe, Somin (2011) obtained the following ages: 364 ± 11 , 368 ± 10 , 387 ± 10 , 390 ± 10 Ma for muscovite, and 366 ± 10 Ma for biotite.

Ca. 10% of the age determinations obtained for zircons from metamorphic rocks and granitoids of the Main Range

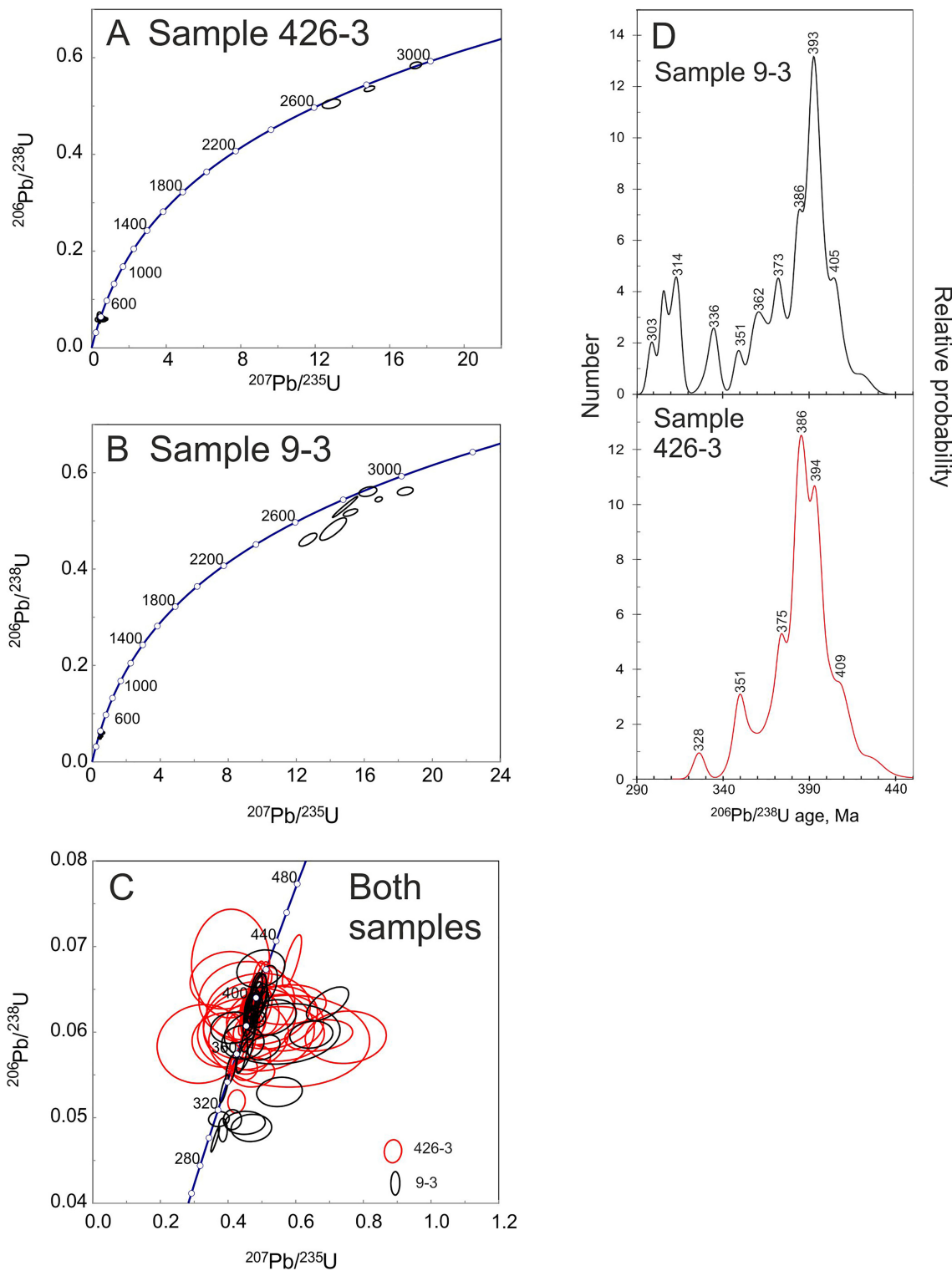
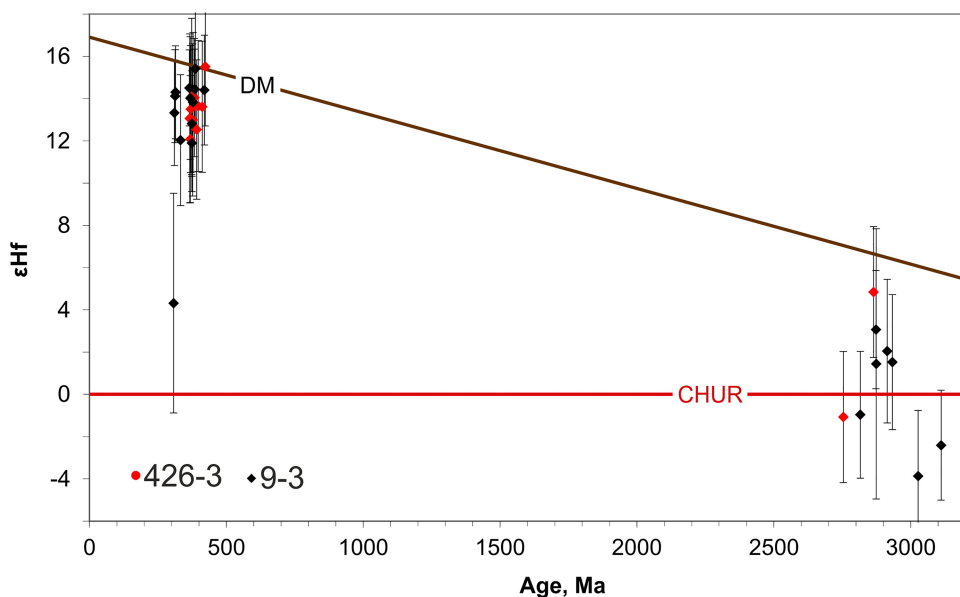


Fig. 6 Results of U-Pb dating of zircon from orthogneisses of the Kamenistaya (**A** sample 426-3) and Beshta (**B** sample 9-3) massifs; **C** results of zircon dating, the young population, both samples; **D** probability density plot of $^{206}\text{Pb}/^{238}\text{U}$ ages for zircon of the young population from two samples

structural zone of the Greater Caucasus fall within the age interval of 650–550 Ma, which corresponds to the Cadomian phase (Gamkrelidze et al. 2020). In contrast, we did

not detect any Cadomian zircon ages from the Beshta-Kamenistaya orthogneisses. This indicates that the crystallization and metamorphism of the Beshta-Kamenistaya

Fig. 7 Results of Hf isotope measurements in zircon from orthogneisses of the Beshta (sample 9-3) and Kamenistaya (sample 426-3) massifs



orthogneisses took place not in their current disposition, but in a geologically different location and environment, which once again confirms the allochthonous nature of the Beshta–Kamenistaya intrusive rocks.

Zaridze and Shengelia (1977, 1978a, b) assumed that rocks of the Lashtarak and Adjarka nappes have experienced regional metamorphism at higher pressure conditions, comparatively with the Main Range zone metamorphic rocks. A comparison of the metamorphic ages of these rocks and orthogneisses of the Beshta–Kamenistaya massif with the ages of magmatic and metamorphic rocks of the Main Range zone indicates that they have experienced metamorphism at nearly the same time but under different conditions. This possibly indicates an existence of a pair of metamorphic belts within this zone of the Greater Caucasus. We assume that the external belt is represented by a few fragments of a once wider belt of high-pressure metamorphic rocks. Presumably, their main part was hidden by subsequent tectonic events or buried under a thick sedimentary cover. Later, these rocks were strongly impacted by the Sudetic granitoids.

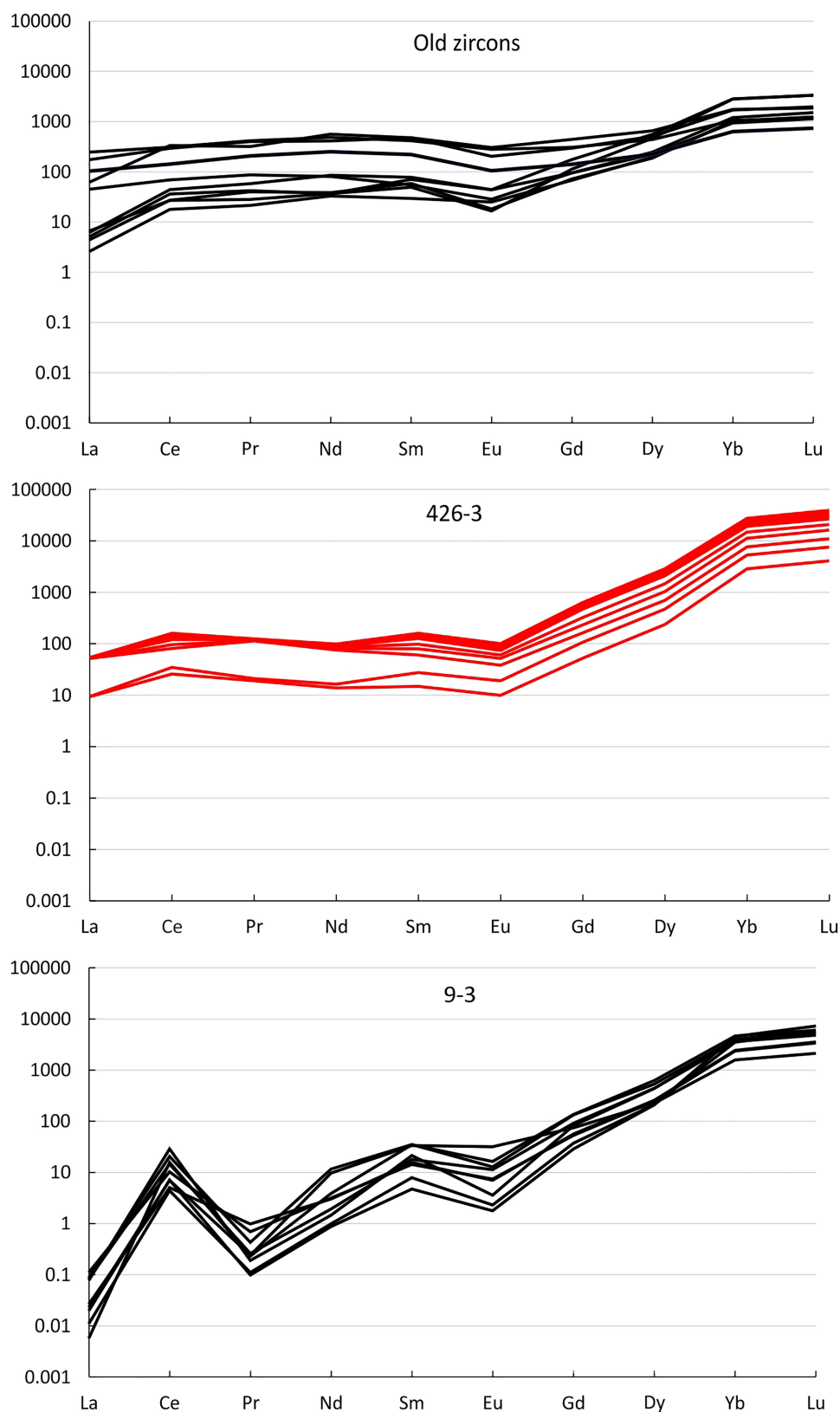
As for the zircon population having the age of 350 Ma and younger, we assume that their origin is related to the emplacement of Sudetic granitoids widespread in the Pass subzone of the Main Range structural zone. As a result of their impact, overgrown rims formed around some zircon grains of the previous generation, but in some zircon grains, rejuvenation took place. The age rejuvenation of zircons is indicated by the presence of ages of 307–299 Ma, since by 310 Ma in the Main Range zone of the Greater Caucasus, magmatic and metamorphic processes had already ended and the basement rocks were overlain by non-metamorphosed Upper Carboniferous–

Permian sediments. In addition, Alpine rejuvenation of micas in the basement rocks of the Greater Caucasus was also established by the data of K–Ar dating (Somin 1971).

The calculation of the SiO₂ composition according to the method proposed by Turner et al. (2020) yielded average values of 53.0% for sample 426-3 and 52.3% for sample 9-3, indicating affinity of the studied zircons to the mafic rocks. The application of the discriminant diagrams proposed by Belousova et al. (2002) also indicates the mafic composition of the source rock. In the discrimination diagram of zircons originated in the oceanic and continental crust (Grimes et al. 2007), zircons of the main population plot in the overlapping area of the oceanic and continental zircons. Finally, zircons of the main population reveal extremely depleted Hf isotope composition, reaching values characteristic of the depleted mantle (Fig. 7). Interestingly, zircons from the Beshta–Kamenistaya massif have more radiogenic Hf isotope composition than coeval zircons megacrysts found in kimberlites in the Azov domain of the Ukrainian Shield ($\epsilon\text{Hf} = 6.8 \pm 0.14$; Shumlyanskyy et al. 2021). All these lines of evidence indicate the affinity of the orthogneisses to the depleted mantle-derived mafic rocks. They may originate due to either igneous fractionation of the mafic melts or remelting of the mafic crust. Most probably they represent oceanic plagiogranites similar to those that associate with basaltic oceanic crust.

Despite the similarity in terms of their age and Hf isotope composition, zircons from the two studied samples differ significantly in terms of REE distribution. Zircons from sample 9-3 have a more fractionated REE pattern and a significant negative Eu anomaly. These data indicate a higher degree of fractionation (including plagioclase

Fig. 8 REE patterns in zircon from orthogneisses of the Beshta (sample 9-3) and Kamenistaya (sample 426-3) massifs



fractionation) compared to sample 426-3. Zircons from sample 9-3 have also a significant positive Ce anomaly,

indicating more oxidizing conditions during their crystallization. Calculation of the oxygen fugacity by applying the

oxybarometer based on trace elements in zircon (Loucks et al. 2020) yielded average $\Delta \log fO_2$ (FMQ) values of -0.6 for sample 426-3 and -1.5 for sample 9-3. These values are in the range typical for the mantle (Frost and McCammon 2008; Dymshits et al. 2020), and mafic layered intrusions (Duchesne et al. 2006). It should be noted that zircons in both studied samples reveal rather wide within-sample variations of $\Delta \log fO_2$ (FMQ) values (Supplementary 3). These can be explained by several factors, that, among others, include internal compositional heterogeneity of individual zircon crystals owing to zoning and heterogeneity in the composition of individual zircon crystals in any rock sample (Loucks et al. 2020). In addition to these factors, we would mention a complex geological history of the studied rocks that resulted in partial chemical exchange with the surrounding minerals.

The second population of zircons in the studied orthogneisses comprises several zircon grains of Mesoarchean to Neoarchean ages. The source of these zircons remains unknown. They crystallized from a melt of intermediate (tonalitic?) composition with average SiO_2 content of 57.6% (according to the method proposed by Turner et al. 2020). These zircons have a relatively flat pattern of REE and high concentrations of LREE, Th, and U. Such peculiarities of their composition are indicative of crystallization from fluid-enriched melts. The calculated applying the oxybarometer of Loucks et al. (2020) average $\Delta \log fO_2$ (FMQ) value for the old zircon population is $+1.6$, which points to reducing conditions during the zircon crystallization.

The origin of the old population of zircon found in both studied samples is unclear. Paleoproterozoic and Archean detrital zircons were sporadically found in the Greater Caucasus in clastogenic rocks (e.g., Somin 2011; Gamkrelidze et al. 2020) and metamorphosed igneous rocks (e.g., Gamkrelidze et al. 2020; Javakhishvili et al. 2021). The presence of such old zircons in metaigneous rocks may indicate the availability of the ancient (Paleoproterozoic—Archean) crystalline basement (or its fragments) in the deep crust in the area (Shumlianska and Burmin 2021).

4 Conclusions

Two age populations of zircons have been distinguished in orthogneisses of the Beshta-Kamenistaya massif based on the data of the LA-ICP-MS U-Pb dating. They are well in line with the geological events stated in this region and show the relation of their formation or transformation with the processes of magmatism and regional metamorphism. The age of zircons of the main population of orthogneisses varies in the interval of 420–300 Ma. Comparable results

gave a Concordia age of 386.9 ± 1.4 Ma, which corresponds to the age of metamorphic recrystallization of orthogneisses in Middle Devonian time during Branderburg orogeny. As for the peaks 375–373 Ma, they also correspond to the ages of regional metamorphic events. Zircons, dated in the Beshta-Kamenistaya intrusion at 350 Ma and younger, correspond to the Late Variscan orogeny and possibly experienced Pb-loss in response to the emplacement of Sudetic granites widespread in the study area. As for zircons that yielded the ages of 3102–2769 Ma, they are xenocrysts that were captured during the formation of initial melts of orthogneisses. Hafnium isotope composition and trace element abundances in the studied zircon indicate the affinity of the orthogneisses to the depleted mantle-derived mafic rocks. They may represent the result of fractionation of the mafic melts or remelting of the mafic crust. Most probably they are oceanic plagiogranites, which is similar to those that associate with basaltic oceanic crust.

Supplementary Information The online version contains supplementary material available at <https://doi.org/10.1007/s11631-022-00558-7>.

Acknowledgements Dedicated to the heroic struggle of the Ukrainian people against Russian aggression. We acknowledge the Curtin Research Office for providing support to LS. The paper has benefitted from constructive comments from Prof. Dr. Chun-Ming Wu (UCAS, University of Chinese Academy of Sciences) and an anonymous reviewer.

Declarations

Conflict of interest All the authors declare that they have no significant competing financial, professional or personal interests that might have influenced the performance of the work described in the manuscript.

References

- Adamia Sh (1984) Pre-Alpine basement of the Caucasus—composition, structure, formation. In: Otkhmezuri Z (ed) Tectonics and metallogeny of the Caucasus. Metsniereba, Tbilisi, pp 1–104 (**in Russian**)
- Baranov G, Grekov I (1982) Geodynamic model of the Greater Caucasus. In: Muratov M (ed) Problems of the geodynamics of the Caucasus. Nauka, Moscow, pp 51–59 (**in Russian**)
- Baranov G, Kropachov S (1976) Stratigraphy, magmatism and tectonics of the Greater Caucasus Precambrian and Paleozoic stages. Nedra, Moscow
- Belousova E, Griffin WL, O'Reilly SY, Fisher NL (2002) Igneous zircon: trace element composition as an indicator of source rock type. Contrib Mineral Petrol 143:602–622. <https://doi.org/10.1007/s00410-002-0364-7>
- Bouvier A, Vervoort JD, Patchett PJ (2008) The Lu-Hf and Sm-Nd isotopic composition of CHUR: constraints from unequilibrated chondrites and implication for the bulk composition of terrestrial planets. Earth Planet Sci Lett 273:48–57. <https://doi.org/10.1016/j.epsl.2008.06.010>

- Coleman R (1977) Ophiolites. Springer, Berlin
- Duchesne JC, Shumlyanskyy L, Charlier B (2006) The Fedorivka layered intrusion (Korosten pluton, Ukraine): an example of highly differentiated ferrobasaltic evolution. *Lithos* 89:353–376
- Dymshits A, Sharygin I, Liu Z, Korolev N, Malkovets V, Alifirova T, Yakovlev I, Xu YG (2020) Oxidation state of the lithospheric mantle beneath Komsomolskaya–Magnitnaya Kimberlite pipe, Upper Muna Field, Siberian Craton. *Minerals* 10:740. <https://doi.org/10.3390/min10090740>
- Frost DJ, McCammon CA (2008) The redox state of Earth's mantle. *Annu Rev Earth Planet Sci* 36:389–420. <https://doi.org/10.1146/annurev.earth.36.031207.124322>
- Gamkrelidze I (1980) On the study of the tectonic nappes of the Caucasus. *Sooobshnya Acad Sci GSSR* 98(2):369–372 (in Russian)
- Gamkrelidze I, Shengelia D (2005) Precambrian-paleozoic regional metamorphism, granitoid magmatism and geodynamics of the Caucasus. Nauchny Mir, Moscow
- Gamkrelidze I, Shengelia D, Chichinadze G (1996) Makera nappe in the crystalline core of the Greater Caucasus and its geological significance. *Bull Georg Acad Sci* 154(1):84–89 (in Russian)
- Gamkrelidze I, Shengelia D, Chichinadze G, Yuan HL, Okrostsvardze A, Beridze G, Vardanashvili K (2020) U–Pb LA–ICP–MS dating of zoned zircons from the Greater Caucasus pre-Alpine crystalline basement: evidence for Cadomian to Late Variscan evolution. *Geologica Carpatica* 71(3):249–263
- Grimes CB, John BE, Kelemen PB, Mazdab FK, Wooden JL, Cheadle MJ, Hanghøj K, Schwartz JJ (2007) The trace element chemistry of zircons from oceanic crust: a method for distinguishing detrital zircon provenance. *Geology* 35:643–646. <https://doi.org/10.1130/G23603A.1>
- Jackson S, Pearson N, Griffin W, Belousova E (2004) The application of laser ablation-inductively coupled plasma-mass spectrometry to in situ U–Pb zircon geochronology. *Chem Geol* 211:47–69
- Javakhishvili I, Shengelia D, Shumlyanskyy L, Tsutsunava T, Chichinadze G, Beridze G (2021) Metamorphism of the Dizi Series rocks (the Greater Caucasus): petrography, mineralogy and evolution of metamorphic assemblages. *Baltica* 34(2):185–202. <https://doi.org/10.5200/baltica.2021.2.5>
- Korikovsky S, Shengelia D, Somin M (1991) Model of pre-Alpine zoned metamorphism of the Greater Caucasus. In: Korikovsky SP (ed) Petrology of the metamorphic complexes of the Greater Caucasus. Nauka, Moscow, pp 216–222 (in Russian)
- Loucks RR, Fiorentini ML, Henríquez GJ (2020) New magmatic oxybarometer using trace elements in zircon. *J Petrol* 61:egaa034. <https://doi.org/10.1093/petrology/egaa034>
- Patchett P, Tatsumoto M (1980) Lu–Hf total-rock isochron for the eucrite meteorites. *Nature* 288:571. <https://doi.org/10.1038/288571a0>
- Potapenko Yu, Stukalina G (1971) First finding of fossils in the Main Caucasian Range metamorphic complex. *Doklady Acad Sci* 198:1161–1162
- Shengelia MD (1987) Regularities of P–T parameters of the Lashtrak tectonic slice regional metamorphism on the basis of its microprobe analysis. *Bull Acad Sci GSSR* 126(3):585–588
- Shengelia MD, Hatar L (1989) Evolution of regional metamorphism of the Sophian uplift (the Greater Caucasus). *Geologica Carpathica* 38(4):457–473
- Shengelia D, Ketskhoveli D (1982) Regional metamorphism of low and moderate pressures in Abkhazia. *Tr GIN AN GSSR* 78:1–206 (in Russian)
- Shengelia D, Chichinadze G, Ketskhoveli D, Mgaloblishvili I, Kakhadze R, Poporadze N (1984) New data on the Atsgara nappe in the Northern Caucasus. *Doklady Acad Sci USSR* 274(6):1450–1453
- Shengelia D, Chichinadze G, Ketskhoveli D, Mgaloblishvili I, Kakhadze R, Poporadze N, Tsutsunava T, Shengelia MD (1986) Petrology of Metamorphites of the Atsgara Nappe in the Northern Caucasus. *Izvestya Acad Sci USSR Geol Ser* 5:17–27 (in Russian)
- Shengelia D, Chichinadze G, Okrostsvardze A (1989) New data on plagiogranite gneisses of the Beshta and mount Kamenistaya (upper Abkhazia). *Bull Acad Sci GSSR* 135(2):393–396 (in Russian)
- Shengelia D, Chichinadze G, Tsutsunava T, Beridze G, Javakhishvili I (2020) On the regional metamorphism of pre-Variscan orthogneisses of Beshta and Mount Kamenistaya inlier. *Janelidze Inst Geol Proc* 132:26–36 (in Georgian)
- Shumlanska LO, Burmin VY (2021) Earthquake focal mechanisms and geodynamic modeling of the Northern and Central Caucasus. *Probl Eng Seismol* 48(4):89–113. <https://doi.org/10.21455/VIS2021.4-5>
- Shumlyanskyy LV, Kamenetsky VS, Tsymbal SM, Wilde SA, Nemchin AA, Ernst RE, Shumlanska LO (2021) Zircon megacrysts from Devonian kimberlites of the Azov Domain, Eastern part of the Ukrainian Shield: Implications for the origin and evolution of kimberlite melts. *Lithos* 406–407:106528. <https://doi.org/10.1016/j.lithos.2021.106528>
- Sláma I, Košler J, Condon D, Crowley J, Gerdes A, Hanchar J, Horstwood M, Morris G, Nasdala L, Norberg N, Schaltegger U, Schoene B, Tubrett M, Whitehouse M (2008) Plešovice zircon—a new natural reference material for U–Pb and Hf isotopic microanalysis. *Chem Geol* 249:1–35
- Söderlund U, Patchett JP, Vervoort JD, Isachsen CE (2004) The ^{176}Lu decay constant determined by Lu–Hf and U–Pb isotope systematics of Precambrian mafic intrusions. *Earth Planet Sci Lett* 219:311–324. [https://doi.org/10.1016/S0012-821X\(04\)00012-3](https://doi.org/10.1016/S0012-821X(04)00012-3)
- Somin ML (1971) Pre-Jurassic basement of the Main Range of the Southern Slope of the Greater Caucasus. Nauka, Moscow
- Somin ML (2011) Pre-Jurassic basement of the Greater Caucasus: a brief overview. *Turkish J Earth Sci* 20:545–610
- Stern R, Bodorkos S, Kamo S, Hickman A, Corfu F (2009) Measurement of SIMS instrumental mass fractionation of Pb isotopes during zircon dating. *Geostand Geoanal Res* 33:145–168
- Turner S, Wilde S, Wörner G, Schaefer B, Lai YJ (2020) An Andesitic source for Jack Hills Zircon supports onset of plate tectonics in the Hadean. *Nat Commun* 11:1241. <https://doi.org/10.1038/s41467-020-14857-1>
- Whitney D, Evans B (2010) Abbreviations for names of rock-forming minerals. *Am Miner* 95:185–187
- Zaridze G, Schengelia D (1977) Metamorphismus, granitoidbildung und plattektonic in Grossen Kaukasus. *Acta Geologica Acad Sci Hungaricae* 21(1–3):99–103
- Zaridze G, Schengelia D (1978) Über Kritallisations differentiation und metasomatische granitization bei der bildung der granitmetamorphit-schicht. *Zeitschrift Fur Geologische Wissenschaften Berlin* 8–9:985–994
- Zaridze G, Shengelia D (1978) Hercynian magmatism and metamorphism of the Great Caucasus in the tight of plate tectonics. *Bull Soc Geol France* VXX 3:355–359

Springer Nature or its licensor holds exclusive rights to this article under a publishing agreement with the author(s) or other rightsholder(s); author self-archiving of the accepted manuscript version of this article is solely governed by the terms of such publishing agreement and applicable law.